ACS APPLIED POLYMER MATERIALS

pubs.acs.org/acsapm Article

Enhancing the Separation Performance of Aqueous Phase Separation-Based Membranes through Polyelectrolyte Multilayer Coatings and Interfacial Polymerization

Muhammad Irshad Baig, Joshua D. Willott, and Wiebe M. de Vos*

Cite This: *ACS Appl. Polym. Mater.* 2021, 3, 3560−3568 Read Online

ACCESS | Metrics & More | Article Recommendations | Supporting Information

ABSTRACT: The aqueous phase separation (APS) technique allows membrane fabrication without use of unsustainable organic solvents, while at the same time, it provides extensive control over membrane pore size and morphology. Herein, we investigate if polyelectrolyte complexation-induced APS ultrafiltration membranes can be the basis for different types of nanofiltration membranes. We demonstrate that APS membranes can be used as support membranes for functional surface coatings like thin polyelectrolyte multilayer (PEMs) and interfacial polymerization (IP) coatings. Three different PEMs were fabricated on poly(sodium 4-styrene sulfonate) (PSS) poly(allylamine hydrochloride) (PAH) APS ultrafiltration membranes, and only 4.5 bilayers were needed to create nanofiltration membranes with molecular weight cut-off (MWCO) values of 210−390 Da while maintaining a roughly constant water permeability (~1.7 $L{\cdot}m^{-2}{\cdot}h^{-1}{\cdot}bar^{-1}$). The PEM-coated membranes showed excellent $MgCl_2$ (~98%), NaCl (~70%), and organic micropollutant retention values (>90%). Similarly, fabricating thin polyamide layers on the ultrafiltration PSS-PAH APS membranes by IP resulted in nanofiltration membranes with MWCO values of ~200 Da. This work shows for the first time that APS membranes can indeed be utilized as excellent support membranes for the application of functional coatings without requiring any form of pretreatment.

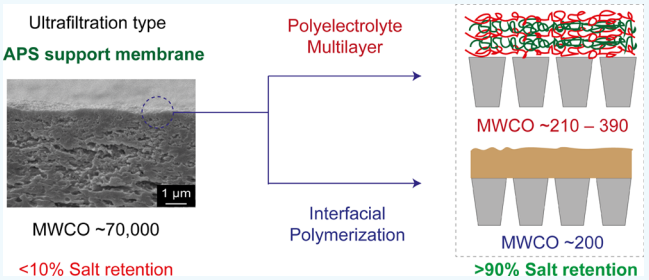

KEYWORDS: *aqueous phase separation membranes, polyelectrolyte multilayer, interfacial polymerization, coatings, nanofiltration*

1. INTRODUCTION

Membrane technology is gradually moving toward greener and more sustainable production techniques.[1,2] In this regard, aqueous phase separation (APS) has been introduced as one of the more sustainable approaches to produce polymeric membranes. This new approach eliminates the use of reprotoxic organic solvents, such as *N*-methylpyrrolidone, the most commonly used organic solvent in the nonsolvent-induced phase separation (NIPS) process. Instead, APS makes use of water as the solvent and nonsolvent to achieve phase separation. Currently, there are two commonly applied APS methods. The first makes use of water-soluble pH-responsive polyelectrolytes where the phase separation is achieved by simply changing the pH of the cast film containing only one type of polyelectrolyte such as poly(4-vinylpyridine)[3] or polystyrene-*alt*-maleic acid copolymers.[4] Membranes ranging from the microfiltration type to dense nanofiltration type can be successfully prepared using this method.

The second APS method uses a mixture of two polyelectrolytes, i.e., a polyanion and a polycation, to obtain a polyelectrolyte complex (PEC) membrane. Sadman et al. utilized this method to produce porous PEC membranes using coacervates of poly(styrene sulfonate) (PSS) and poly(*N*-ethyl-4-vinylpyridinium) (QVP-C2).[5] The PSS-QVP-C2 membranes presented in their work demonstrated a good water flux, organic solvent stability, and excellent rejection of polystyrene beads of ~100 nm in size. However, this polyelectrolyte system had its own limitations as membrane fabrication protocols are at times lengthy, while the control over the membrane pore size was limited. In another instance, Durmaz et al. obtained dense nanofiltration type PEC membranes having a molecular weight cut-off of <300 Da using a solution of PSS and poly(diallyldimethylammonium chloride) (PDADMAC) that was prepared at high salt concentrations and precipitated in deionized water.[6] This method is also known as the "salinity change-induced APS" because the phase separation is achieved by lowering the salt concentration in the polyelectrolyte solution, thereby forming a PEC membrane. A similar method was also applied by Kamp et al. to produce ultrafiltration and nanofiltration type PSS−PDADMAC membranes.[7] However,

Received: April 13, 2021
Accepted: June 14, 2021
Published: June 18, 2021

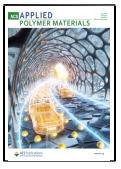

the downsides of these PSS-PDADMAC membranes in both studies are the relatively lower water permeabilities, i.e., ∼0.1 to 1 $L \cdot m^{-2} \cdot h^{-1} \cdot bar^{-1}$ and the limited control over the membrane pore size. Another interesting method is the "pH shift-induced APS" where a polycation and polyanion solution is prepared at high pH and precipitated in low pH conditions (or vice versa) to achieve phase separation. In previous studies, we have successfully employed this method to obtain PEC membranes with tunable pore sizes ranging from microfiltration to nanofiltration using a mixture of PSS−poly(allylamine hydrochloride) (PAH) and also PSS−polyethyleneimine (PEI).[8−10] While the pore size of the PSS-PAH membranes could be controlled from ∼200 to ∼2 nm, dense nanofiltration membranes were not obtained.[8] The open nanofiltration (or tight ultrafiltration) type PSS-PAH membranes obtained in our earlier study did not show any significant retention of salts and showed only ∼80% average retention of a range of organic micropollutants. For most nanofiltration applications, the membranes need to be able to retain salts and organic micropollutants in excess of 90%. Similarly, in another work by Durmaz et al. on "pH shift-induced APS", PSS and poly(acrylic acid) (PAA) were used to obtain only microfiltration type PEC membranes.[11]

Traditionally, most dense membranes, such as nanofiltration and reverse osmosis membranes, are based on porous support membranes prepared by NIPS and subsequently coated with thin layers of another material. In a similar fashion, it stands to reason that porous APS membranes can and should be used as support membranes in a similar fashion.

Numerous coating strategies are available in the literature to improve the performance of polymeric membranes in terms of their water flux, selectivity, chemical resistance, mechanical properties, and antifouling ability.[12] Among them, one of the most commonly applied is interfacial polymerization (IP) where a thin polyamide film is coated on the membrane surface via a reaction of two or more monomers such as *m*-phenylenediamine (MPD) in the aqueous phase and trimesoyl chloride (TMC) in the organic phase.[13] Over the years, IP has been well-studied in terms of the types of monomers, the concentrations of the monomers, and other reaction conditions to obtain thin-film composite (TFC) and nanocomposite membranes.[13−19] TFC membranes obtained via IP typically have excellent salt retentions[20,21] and chemical/physical stability[22] and are still the most preferred option for commercial nanofiltration membranes.

In recent years, another interesting coating approach that utilizes polyelectrolytes has gained significant attention. The so-called layer-by-layer (LBL) approach was first described by Decher to obtain self-assembled polyelectrolyte multilayers (PEMs) by alternatively coating polycations and polyanions on solid supports.[23] This process can be used to prepare thin layers (usually 10−50 nm) on the surface of charged porous support membranes due to electrostatic interactions of the oppositely charged polyelectrolytes.[24] The PEM approach has proven to be a very versatile method to obtain ultrathin and dense coatings because of the ability to fine-tune their properties through, for example, the number of bilayers, salt concentration, and the pH of the coating solutions.[25−27] In addition, the PEM-coated membranes have also shown excellent chemical stability and resistance against cleaning/backwashing processes.[28] Common and successful PEM coatings include PSS-PDADMAC, PSS-PAH, PAA-PAH, and PSS-PEI.[25] Each polyelectrolyte pair has different properties and performances, and this can be further fine-tuned by controlling the coating process. For instance, PSS-PAH multilayer coatings have a lower polyelectrolyte mobility and typically show a higher water permeability with good salt retentions.[29] The PSS-PDADMAC multilayer coatings show excellent physical and chemical stability against back flushing[30] and show a particularly high anion selectivity toward sulfate and phosphate.[31,32] On the other hand, PSS-PEI multilayer coatings form dense complexes and therefore show relatively lower water permeabilities but with excellent salt and organic molecule retentions.[33] In addition, the PSS-PAH and PSS-PDADMAC multilayer coatings have the polycation in excess in bulk and therefore are more susceptible to swelling.[33] In comparison, the PSS-PEI coatings have significantly less excess of polycation and therefore have less degree of swelling.

In this work, we use the advantages of PEM and IP coatings and demonstrate that APS-based membranes can also act as excellent supports for these functional coatings. One of the major advantages of using APS membranes for PEM coatings is the inherent charge of these membranes, which facilitates the adsorption of charged polyelectrolytes. We have shown in our earlier work that PSS-PAH-based APS membranes have positive charge on their surface.[8] As a result, these support membranes can be directly coated with a layer of polyanions without any pretreatment processes. Similarly, the excess amount of PAH in the PSS-PAH support membranes provides amine groups that can take part in the IP process by reacting with the TMC, thereby improving the adhesion of the IP layer to the support membrane. In this work, the support PSS-PAH-based APS membranes are prepared following the protocols extensively discussed in our earlier work.[8] PEM coatings are performed using three different polyelectrolyte pairs, i.e., PSS-PAH, PSS-PDADMAC, and PSS-PEI. Figure 1 shows the chemical structures of these polyelectrolytes. The multilayer membranes are coated on the APS support membranes to

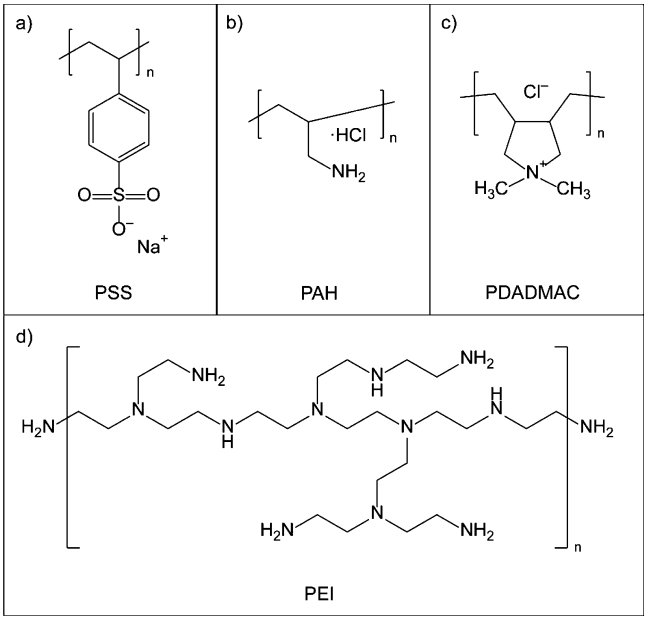

Figure 1. Chemical structures of the polyelectrolytes used for performing PEM coatings on the APS membrane supports. (a) Poly(sodium 4-styrene sulfonate) (PSS), (b) poly(allylamine hydrochloride) (PAH), (c) poly(diallyldimethylammonium chloride) (PDADMAC), and (d) branched polyethyleneimine (PEI).

https://doi.org/10.1021/acsapm.1c00457
ACS Appl. Polym. Mater. 2021, 3, 3560−3568

densify the top surface structure and provide the membranes with nanofiltration performance. Similarly, IP was performed on porous (ultrafiltration) PSS-PAH membranes and the IP reaction conditions were optimized to obtain stable TFC membranes. Finally, all the coated membranes are tested for their nanofiltration performance using a range of different salts and organic micropollutants. This study showcases the versatility of APS membranes by demonstrating that they can function as support membranes for a multitude of surface coatings without requiring any pretreatment.

2. EXPERIMENTAL SECTION

2.1. Materials. The chemicals PSS (30 wt % with $M_w \sim 200$ kDa and 25 wt % with $M_w \sim 1000$ kDa), PDADMAC (20 wt %, $M_w \sim 200-350$ kDa), PEI (50 wt %, $M_w \sim 750$ kDa), sodium hydroxide (NaOH, >98%), sodium chloride (NaCl, >99.5%), hydrochloric acid (HCl, 37%, ACS reagent), glutaraldehyde (GA, 50 wt %), glycerol solution (86−89 wt %), MPD (99%), 1,3,5-benzenetricarbonyl trichloride (98%, TMC), *n*-hexane (≥99%), magnesium sulfate ($MgSO_4$, >99.5%), sodium sulfate (Na_2SO_4, 99%), magnesium chloride hexahydrate ($MgCl_2.6H_2O$, ≥99%), sodium chloride (NaCl, >99.5%), polyethylene glycol (PEG) with different molecular weights (M_w 200, 400, 600, 1500, and 2000 g·mol^{-1}), atrazine (analytical standard), atenolol (>98%), bezafibrate (>98%), bromothymol blue (>95%), bisphenol-A (>99%), naproxen (analytical standard), phenolphthalein (analytical standard), and sulfamethoxazole (analytical standard) were purchased from Merck (The Netherlands). PAH (40 wt %, $M_w \sim 150$ kDa) was purchased from Nittobo Medical Co. Ltd., Japan. Deionized water was obtained from a Milli-Q Ultrapure water purification system.

2.2. Membrane Fabrication. The PEC membranes were prepared using recipes reported in our earlier work.[8] Briefly, first, a 25 wt % PSS ($M_w \sim 1000$ kDa) solution was diluted to 12 wt % using deionized water. Second, 40 wt % PAH ($M_w \sim 150$ kDa) was diluted to 12 wt % by the addition of deionized water and 10 M NaOH solution. The NaOH solution was added such that the ratio of wt % NaOH to wt % PAH was constant at 0.5. The reason to add NaOH is to increase the pH of the aqueous PAH solution to ∼14, thereby making it uncharged so that it can be mixed with PSS without forming a PEC. Finally, the 12 wt % PSS and PAH solutions were mixed in a monomer mixing ratio of PSS to PAH of 1:2. The ratios are based on the monomer weight of the polyelectrolytes, i.e., ∼206 g·mol^{-1} for PSS and ∼93.5 g·mol^{-1} for PAH. This ratio of polyelectrolytes was selected because it results in mechanically stable membranes.[8] The casting solution was constantly stirred until it became homogeneous.

The solution was then cast as a thin film on a glass plate using a casting bar having a gap of 0.6 mm. To obtain the open nanofiltration type membrane supports for multilayer coatings, the cast solution was immediately immersed in a coagulation bath at pH 1 (adjusted using HCl) containing 0.05 wt % GA and 4 M NaCl. This composition of the coagulation bath was chosen because it results in open nanofiltration type PSS-PAH membranes as mentioned in our previous work.[8] Here, GA is used as a cross-linking agent for the amines of PAH, while NaCl facilitates the polyelectrolyte chain rearrangement resulting in a denser complex. On the other hand, the ultrafiltration type membrane supports for IP were obtained by immersing the PSS-PAH cast films in a coagulation bath at pH 1 (adjusted using HCl) containing 0.05 wt % GA without any NaCl. The cast films immediately precipitated at low pH and turned opaque. The films were then removed from the bath after 24 h and kept in deionized water for further use.

2.3. Multilayer Coatings. Three different types of multilayer coatings were applied in this work, i.e., PSS-PAH, PSS-PDADMAC, and PSS-PEI. The coating solutions contained 1 g·L^{-1} of polyelectrolyte (polyanion or polycation) in 500 mM NaCl solution. This concentration of NaCl was chosen because thicker multilayer coatings are obtained at higher salt concentrations because of the increased extrinsic charge compensation within the multilayers.[34] The pH of all the polyelectrolyte solutions was set to 6 by adding 0.1 M NaOH/HCl. PSS and PDADMAC are strong polyelectrolytes, meaning that the pH of the solution has no impact on their charge. On the other hand, PAH and PEI are weak polyelectrolytes whose charge is dependent on the pH of the solution. It is known from the literature that PSS-PAH multilayer membranes when coated at pH 6 form dense PEMs that show high retention of organic micropollutants.[35] Therefore, pH 6 was chosen as the coating solution pH for performing multilayer coatings. The multilayers were built using the following protocol. The support membranes were first soaked in 500 mM NaCl solution for 15 min followed by a 15 min dip coat in 1 g·L^{-1} PSS (polyanion, $M_w \sim 200$ kDa) solution. Afterward, the membranes were taken out and immediately washed in three steps with 500 mM NaCl solution for 15 min each. The membranes were then dipped in 1 g·L^{-1} polycation (either PAH, PDADMAC, or PEI) solution for 15 min followed by a three-step wash in 500 mM NaCl solution for 15 min each. This process produced one bilayer. The procedure was repeated to obtain 4.5 bilayers of each PSS-PAH, PSS-PDADMAC, and PSS-PEI with PSS as the ending layer. The PEM membranes with 4.5 bilayers are referred to as PSS-PAH$_{(4.5)}$, PSS-PDADMAC$_{(4.5)}$, and PSS-PEI$_{(4.5)}$. The coated flat sheet membranes were stored in deionized water for further usage.

2.4. IP. IP was carried out using MPD and TMC as monomers. A 2 wt % MPD solution was prepared in deionized water and stirred until it became homogeneous. A 0.2 wt % TMC solution was prepared by dissolving TMC in *n*-hexane. The IP coating was then applied on the ultrafiltration type PSS-PAH membranes using the following protocol. First, the membranes were immersed in the aqueous MPD solution for 10 min. When the membranes were taken out, they appeared shiny due to the presence of water on the surface, which was removed by means of a rubber roller. Afterward, the membranes were vertically dried inside an aerated fume hood until they appeared dry and dull.[13] The MPD saturated membrane supports were then immersed in the TMC solution for 3 min to initiate the IP reaction after which they were dried again in the fume hood for 30s before heat treatment in an oven at 70 °C for 5 min. The membranes were taken out, washed with deionized water, and stored in deionized water for further usage.

2.5. Characterization. Scanning electron microscopy (SEM) was performed with a JSM-6010LA, JEOL, Japan. The membrane samples for SEM were first immersed in a 20 wt % glycerol solution for 4 h and then dried in an aerated fume hood for 24 h. This procedure ensures that the pores of the membranes remain intact. For cross-section images, the dried membrane samples were immersed in liquid N_2 and carefully fractured to reveal the full cross section. All the membrane samples were kept in a vacuum oven at 30 °C for 24 h before sputter coating them with a 5 nm thin layer of Pt/Pd alloy using a sputter coater Quorum Q150T ES (Quorum Technologies, Ltd., UK). Fourier transform infrared (FTIR) spectroscopy was conducted using a Spectrum Two (Perkin Elmer, USA) in attenuated total reflectance mode in the wavenumber range 600 to 4000 cm^{-1}.

The charge on the membrane surface was determined at pH 6 using a SurPASS electrokinetic analyzer (Anton Paar, Graz, Austria) by measuring the streaming current versus pressure in a 5 mM KCl solution.

For the pure water permeability (PWP) measurements, the membranes were cut into circular disks having a diameter of 25 mm and then mounted on a dead-end Amicon cell. The exposed surface area of the membranes was ∼3.8 cm^2. The vessel containing the feed water was pressurized to 4 bar using N_2 gas. The permeate mass was measured as a function of time via mass balance connected to a computer. The PWP (P) was calculated using eq 1:

$$P = \frac{J_W}{\Delta p} \tag{1}$$

where J_W is the pure water flux calculated by measuring the change in permeate volume (in liters) per membrane area (3.8 cm^2) over time (h) and Δp is the pressure difference (bar) between the feed and permeate side.

https://doi.org/10.1021/acsapm.1c00457
ACS Appl. Polym. Mater. 2021, 3, 3560−3568

The molecular weight cut-off (MWCO) of the membranes was determined using a feed solution of PEG having different molecular weights, i.e., 200 to 2000 g·mol^{-1}, each at a concentration of 1 g·L^{-1} in water. The mixture was filtered through the membranes in a dead-end cell at 3 bar, and the permeate and retentate samples were collected. The feed, retentate, and permeate were then analyzed via gel permeation chromatography (GPC, Agilent 1200/1260 Infinity GPC/SEC series, Polymer Standards Service data center and column compartment) using Milli-Q water eluent containing 50 mg·L^{-1} NaN_3, at 1 mL·min^{-1}, through a 1000 Å, 10 μm Polymer Standards Service Suprema 8 × 300 mm column and 30 Å, 10 μm column connected in series. GPC determines the concentration of PEGs via refractive index detection. The retention (R) was calculated using eq 2:

$$R = \left[1 - \frac{C_p}{\frac{(C_f + C_r)}{2}}\right] \times 100 \quad (2)$$

where C_p, C_f, and C_r, are the concentrations in the permeate, feed, and retentate side, respectively. Here, an average of feed and retentate concentration is taken because the concentration of the feed solution in a dead-end cell is always changing. A sieving curve of retention vs molecular weight of PEG was plotted, and the MWCO was determined as shown in Figure S4, Supporting Information.

A 5 mM aqueous solution of four different types of salts, i.e., $MgCl_2$, $MgSO_4$, Na_2SO_4, and NaCl, was filtered through the membranes at 4 bar of feed pressure. The feed, retentate, and permeate samples were collected and measured for their conductivity using a handheld WTW Cond 3210 conductivity meter (Xylem Analytics, Germany). A calibration curve was obtained by plotting conductivity as a function of known concentrations of salt solutions. Consequently, the concentration of either type of salt in the actual feed, retentate, and permeate was determined according to the calibration curve and the retention was calculated using eq 2.

A cocktail mixture of eight different types of micropollutants was prepared by dissolving 3 mg·L^{-1} of each micropollutant in deionized water followed by adjusting the solution pH to 5.8 using 0.1 M NaOH. At this pH, the micropollutants are either positively charged, negatively charged, or neutral. Such a diverse combination of micropollutants can provide an assessment on the charge-based and size-based separation of molecules by the membranes. The mixture was filtered through the membranes for 24 h to achieve steady-state permeation before collecting the feed, retentate, and permeate samples. These samples were analyzed using an UltiMate 3000 UHPLC (ThermoFisher Scientific, USA) using a 2.2 μm ACCLAIM RSLC C18 column (ThermoFisher Scientific, USA) for separation. A calibration curve was first obtained using known concentrations of the micropollutant cocktail mixture. The concentrations of micropollutants in the feed, retentate, and permeate were estimated according to the calibration curve obtained using known concentrations of the micropollutant cocktail mixture. The retention was then calculated using eq 2.

3. RESULTS AND DISCUSSION

3.1. Multilayer Coatings. When considering APS-based membranes as supports for PEM coatings, the natural charge of the APS membranes can be considered as a real advantage, allowing easy coatings. The top surface and cross-section SEM images of all three different types of PEM membranes coated with 4.5 bilayers are shown in Figure 2 along with the uncoated APS support membrane. The PSS-PAH$_{(4.5)}$ membranes showed relatively smooth top surfaces as compared to the PSS-PDADMAC$_{(4.5)}$ and PSS-PEI$_{(4.5)}$, see Figure 2c,e,g. It is well known that PSS-PAH multilayers have a lower mobility[29] and a higher number of interactions within the multilayer[36] as compared to the others studied in this work, which could explain the smooth texture of PSS-PAH PEMs. On the other hand, the PSS-PDADMAC- and PSS-PEI-coated membranes exhibited rougher and more uneven surfaces containing aggregates and also some degree of layering (especially in the case of PSS-PEI) as seen in Figure 2e,g. Chen et al. also found similar morphologies for PEMs and concluded that such morphologies could possibly be due to the inhomogeneous charge distribution on the substrate that could lead to isolated deposition of material.[37] However, in the case of PSS-PEI multilayer membranes, the uneven top surfaces could possibly be due to the branched nature of the higher molecular weight PEI, which forms slightly thicker coatings. Nevertheless, the membranes contained no defects, as will be established later by the organic micropollutant retention experiments. The cross-section SEM images of the PEM-coated membranes, shown in Figure 2d,f,h, do not reveal any significant information because it is difficult to estimate the PEM layer thickness via SEM images, especially as the coated material is very similar in nature to the materials of the support membranes. A better estimate of PEM thickness is obtained by utilizing optical fixed-angle reflectometry or ellipsometry. For the systems studied here, these thicknesses have been obtained in literature, coming to estimated thicknesses of ~25 nm for PSS-PDADMAC, ~16 nm for PSS-PEI,[38] and ~20 nm for PSS-PAH.[39]

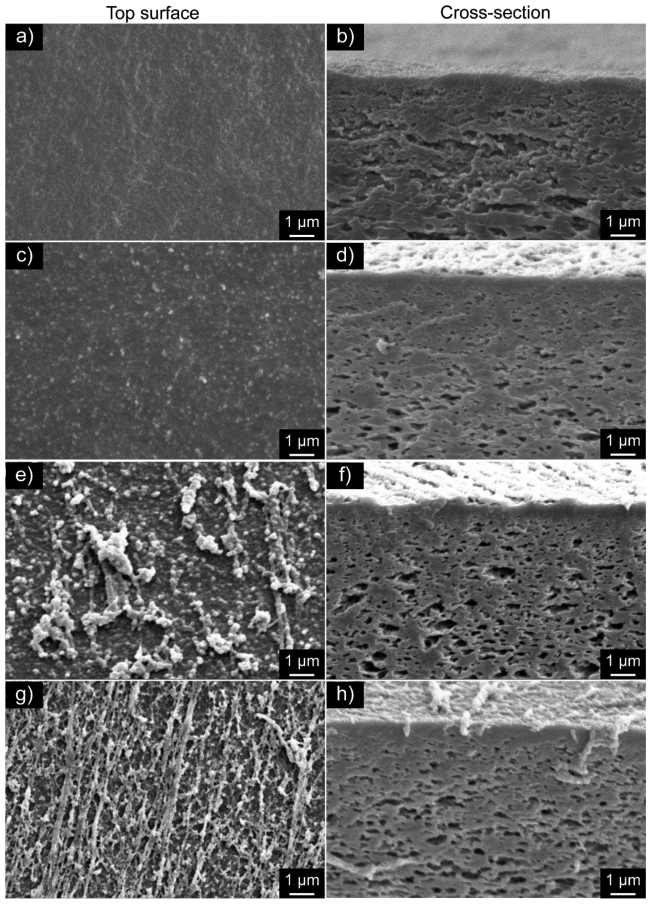

Figure 2. Top surface and cross-section SEM images of (a, b) APS support membrane and the PEM membranes coated with 4.5 bilayers of (c, d) PSS-PAH, (e, f) PSS-PDADMAC, and (g, h) PSS-PEI.

Figure 3a shows the PWP and MWCO of the three different types of PEM-coated membranes. For reference, the PWP of the support APS membranes was ~2 L·m^{-2}·h^{-1}·bar^{-1}. The PWP and salt retentions of the PEM membranes with 1.5 to

https://doi.org/10.1021/acsapm.1c00457
ACS Appl. Polym. Mater. 2021, 3, 3560−3568

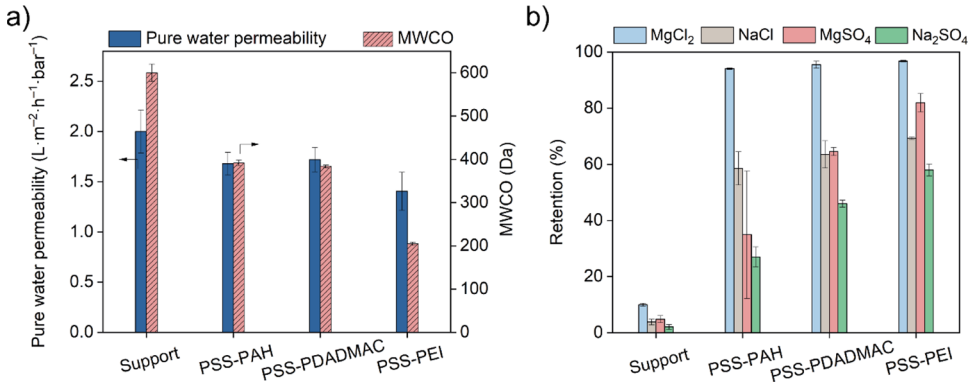

Figure 3. (a) Pure water permeability and molecular weight cut-off. (b) Salt retentions of PSS-PAH$_{(4.5)}$, PSS-PDADMAC$_{(4.5)}$, and PSS-PEI$_{(4.5)}$ membranes. The support membrane showed negligible salt retentions as compared to the enhanced salt retentions by the PEM-coated membranes. The retention tests were conducted at a feed pressure of 4 bar.

3.5 bilayers are show in Figures S1−S3, Supporting Information. For all three PEM coatings, excellent NF performance is observed, a large improvement compared to just the support membrane. However, the three different polyelectrolyte systems do show varying PWP and MWCO values, in accordance with the previous studies.[31] The PWP of PSS-PAH$_{(4.5)}$- and PSS-PDADMAC$_{(4.5)}$-coated membranes was almost similar, i.e., ∼1.7 L·m^{-2}·h^{-1}·bar^{-1}. On the other hand, the PSS-PEI$_{(4.5)}$ membranes showed a lower PWP of ∼1.4 L·m^{-2}·h^{-1}·bar^{-1}. Such a trend is observed because the PSS-PEI multilayer membranes are known to be denser than PSS-PDADMAC and PSS-PAH.[33] For branched PEI, the charge density is higher than that of PDADMAC and PAH. Consequently, the number of ion pairs per number of carbon atoms in the resulting PEC is higher for PSS-PEI$_{(4.5)}$ as compared to the rest. A higher charge density leading to a higher density of ionic crosslinks, coupled with lower excess charge as described in the introduction, usually results in a lower permeation rate.[40] The dense nature of PSS-PEI$_{(4.5)}$ was also confirmed by the MWCO of these PEM membranes. The MWCO of the relatively less dense PSS-PAH$_{(4.5)}$ and PSS-PDADMAC$_{(4.5)}$ was estimated to be ∼392 ± 6 Da and ∼384 ± 3 Da, see Figure S4a,b in the Supporting Information. In comparison, the dense PSS-PEI$_{(4.5)}$ membranes showed a MWCO of ∼205 ± 4, Figure S4c.

The separation performance of the membranes prepared in this work is compared to the commercial membranes in terms of their PWP and the NaCl retention and is presented in Table S1, Supporting Information. The water permeabilities of the APS support membranes (∼2 L·m^{-2}·h^{-1}·bar^{-1}) and the PEM membranes reported here are relatively lower as compared to most commercial membranes used for nanofiltration applications. This is indeed a current limitation of the APS membranes, and future efforts could be devoted toward increasing the PWP of the support membranes. One possible way is to utilize additives such as PEG in the polyelectrolyte casting solution, which is also commonly used for NIPS membranes as the pore former.[41] Nevertheless, the sustainable APS membrane supports show decent salt selectivity while facilitating the PEM formation due to their inherent surface charge.

Figure 3b shows the retention of four different types of salts by the support membrane and the different PEM membranes. The salts that were used for the retention measurements contain both monovalent and divalent anions/cations, which can also give a fair indication of the charge in the bulk of PEM membranes. As expected, the support membrane showed negligible (<10%) retention of the four types of salts. For the PEM membranes, the retention trend follows the permeability data such that the membranes with a lower water permeability showed the higher retentions. PSS-PEI$_{(4.5)}$ showed the highest retention for all four types of salts because of its dense nature. The higher retention of $MgCl_2$ as compared to the other salts is due to the net positive charge on the PEM membrane surfaces, which was confirmed by measuring the surface streaming potential of these membranes. PSS-PAH$_{(4.5)}$ membranes had a streaming potential of ∼9 ± 0.4 mV, PSS-PDADMAC$_{(4.5)}$ ∼9 ± 0.2 mV, and PSS-PEI$_{(4.5)}$ ∼ 4 ± 0.7 mV. The salt retention results indicate that the separation mechanism is most likely to be a combination of the size exclusion and Donnan exclusion mechanisms. A positively charged membrane will repel the cations and attract the anions based on the Donnan exclusion mechanism.[42] The higher rejection of divalent cation Mg^{2+} and a lower rejection of divalent anion SO_4^{2-} are then expected. Looking at the streaming potentials of the three types of membranes, it can be observed that PSS-PEI$_{(4.5)}$ has a relatively lower charge of ∼4 mV as compared to the other two systems. This confirms our earlier statement that PSS-PEI$_{(4.5)}$ has the highest number of ion pairs per number of carbon atoms among the three PEMs resulting in less overall charge and also a more dense layer.

The results clearly indicate that coating a thin layer of PEMs on top of the APS membranes can lead to the formation of excellent nanofiltration type membranes. The versatility of the LBL approach allows further optimization of the membranes' separation performance by simply tuning the number of bilayers, salt concentration, and the pH of the coating solutions.

To further quantify the nanofiltration separation performance of the PEM membranes, a mixture of eight different types of micropollutants was prepared and filtered through the membranes, see Figure S5 in the Supporting Information for the chemical structures of these micropollutants. These micropollutants are mostly pesticides, pharmaceuticals, and plasticizers and are most commonly found in rivers and other ground water sources.[43] The mixture contains both hydrophilic/hydrophobic and charged/uncharged molecules with molecular weights in the range of 200 to 700 Da. Table 1 presents the micropollutant retentions of the PEM membranes studied in this work.

https://doi.org/10.1021/acsapm.1c00457
ACS Appl. Polym. Mater. 2021, 3, 3560−3568

Table 1. Micropollutant Retentions of the PEM Membranes[a]

micropollutant	M_w (Da)	charge	retention (%) PSS-PAH$_{(4.5)}$	PSS-PDADMAC$_{(4.5)}$	PSS-PEI$_{(4.5)}$
atenolol	267	+	60	97	97
atrazine	216	0	50	62	90
bisphenol-A	228	0	50	53	92
phenolphthalein	318	0	75	87	97
bromothymol blue	624	0	100	100	100
sulfamethoxazole	253	0/−	26	30	56
naproxen	229	−	94	95	97
bezafibrate	361	−	89	89	99

[a]The concentration of the mixture was 3 mg·L^{-1} of each compound and the pH was adjusted to 5.8.

As expected, the neutral molecules like atrazine, bisphenol-A, phenolphthalein, and bromothymol blue are highly rejected based on their sizes according to the MWCO of the PEM membranes. Bromothymol blue being the largest molecule (M_w ~ 624 Da) is completely retained by the membranes, also demonstrating that all three membrane types are defect free. The positively charged atenolol shows higher retentions because of the positively charged membrane surface. Overall, the PSS-PAH$_{(4.5)}$ shows an average micropollutant retention of ~68%; that of PSS-PDADMAC$_{(4.5)}$ is ~77%, and that of PSS-PEI$_{(4.5)}$ is ~91%. The results also suggest that the separation of the organic micropollutant is not governed only by size exclusion and Donnan exclusion mechanisms; steric hindrance and dielectric effects are also known to affect the retentions in typical nanofiltration membranes.[44] The separation is likely based on a combination of these mechanisms.

It can certainly be concluded that by only coating 4.5 bilayers of PEMs, the otherwise open nanofiltration type APS membrane can be made into a dense nanofiltration type. The real advantage is that the PEMs can be applied without any pretreatment due to the natural charge of the APS support membranes, which facilitates the adsorption of polyelectrolytes for the multilayer buildup. These results also suggest that PSS-PAH-based APS membranes can be effectively used as supports to build PEM-based membranes with excellent separation properties. It is also pertinent to mention that the aim of this work was not to obtain the best-performing PEM membranes but to show that APS membranes, just like NIPS membranes, can be excellent support membranes for functional coatings.

3.2. IP. IP was carried out on the ultrafiltration type PSS-PAH membranes having an average pore size of ~4.5 nm, calculated in our earlier work.[8] The existence of the IP coated polyamide layer was confirmed by FTIR spectra shown in Figure 4.

In the case of the PSS-PAH support membrane, the sharp absorbance bands at 1008, 1036, and 1123 cm^{-1} and the overlapping bands at 1180 and 1208 cm^{-1} are assigned to the S═O stretching modes in PSS.[45] Other characteristic peaks of PSS appear at 1601, 1495, 1453, and 1411 cm^{-1}, all of which are assigned to the aromatic −C═C− stretching. The relatively less prominent peaks observed in the IR spectra of the support membranes at 1603 and 1522 cm^{-1} can be assigned to asymmetric and symmetric vibrations of $-NH_3^+$, respectively.[46]

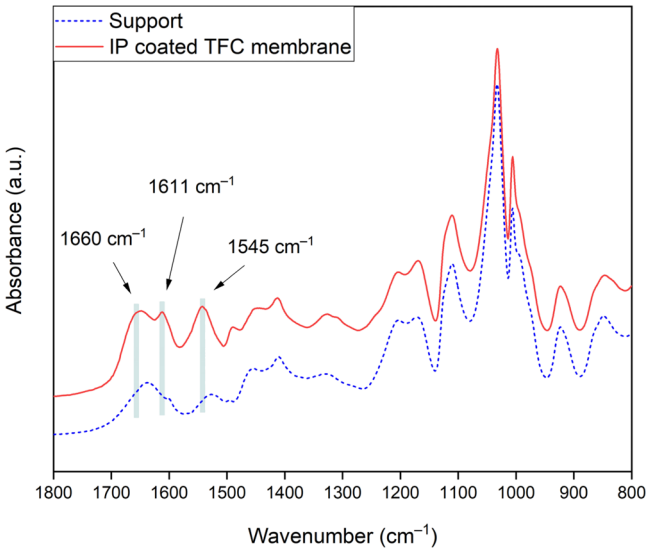

Figure 4. FTIR spectra of the ultrafiltration type PSS-PAH support and the IP coated thin-film composite (TFC) membrane. The appearance of absorbance bands at 1545, 1611, and 1660 cm^{-1} confirms the presence of polyamide in TFC membranes.

The FTIR spectra of the IP coated TFC membrane showed additional bands at 1660 cm^{-1} (C═O stretching vibrations in amide I), 1611 cm^{-1} (aromatic ring breathing, N−H bending/stretching, amide II), and 1545 cm^{-1} (C−N stretching of amide), all of which are characteristic polyamide bands.[47] The FTIR spectra reveal that the PSS-PAH support membranes are indeed coated with a thin layer of polyamide.

The SEM images of the pristine support membrane and the TFC membrane are shown in Figure 5. Comparing SEM images in Figure 5a,b, it can be seen that the TFC membrane had a slightly rough top surface with a typical leaflike morphology that is most associated with a polyamide layer.[48]

The difference between the pristine support and the TFC membrane is evident by looking at the cross-section SEM images in Figure 5. The PSS-PAH support membrane shows an asymmetric structure with the pore size getting larger as you move from top to bottom of the cross section, see Figure 5c. On the other hand, the TFC membrane has a relatively denser and more closed structure at the given magnification, Figure 5d. This indicates that the polyamide layer has reduced the pore size and/or completely closed the pores near the membrane top surface. This happens because upon immersing the porous support membrane in the MPD solution, the near surface pores are completely filled with the aqueous solution. The MPD molecules remain inside the pores even after drying with a rubber roller. When the support is subsequently immersed in the organic TMC solution, the MPD molecules diffuse toward the organic front because of their higher solubility in the organic solvent and immediately react with TMC to form polyamide nuclei. The newly formed nuclei grow laterally until they combine with other nuclei to form a polyamide layer.[13] The diffusion of MPD molecules and the subsequent reaction with TMC gives rise to the typical leaflike morphology associated with the polyamide layer.

The charge on the TFC membrane surface was determined to be approximately −35 ± 0.5 mV at pH 6. The polyamide layer is negatively charged because of the dissociation of the carboxyl groups.[49] The negatively charged TFC membrane is thus expected to have high retentions of divalent anions.

https://doi.org/10.1021/acsapm.1c00457
ACS Appl. Polym. Mater. 2021, 3, 3560−3568

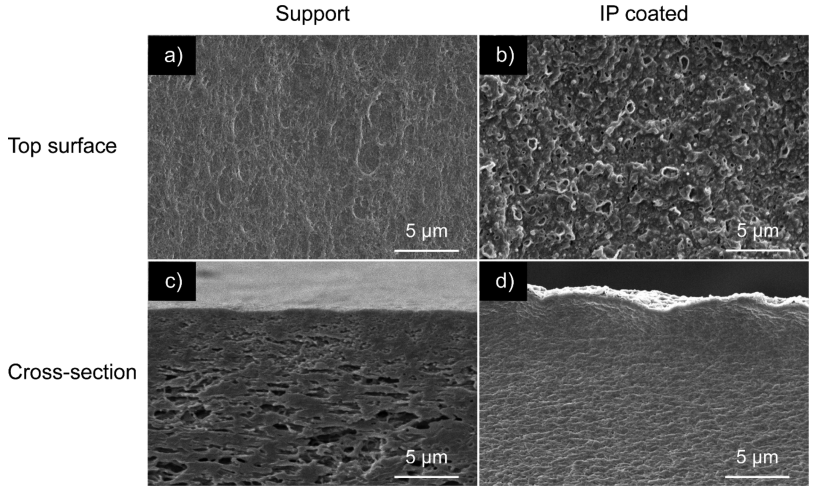

Figure 5. Top surface and cross-section SEM images of the (a and c) APS support membrane and (b and d) IP coated membrane.

The PWP at 4 bar of applied water pressure was measured for the TFC membrane. In comparison with the support membrane, which had a permeability of ~12.5 $L \cdot m^{-2} \cdot h^{-1} \cdot bar^{-1}$, the TFC membranes showed a significantly lower water permeability of ~1.1 $L \cdot m^{-2} \cdot h^{-1} \cdot bar^{-1}$. This is fully expected behavior because the TFC membrane is significantly denser than the support membrane, and therefore, there is higher resistance to the passage of water, see Figure 5c,d. The MWCO of the IP coated TFC membranes was measured to be ~200 ± 3 Da.

The nanofiltration performance of the membrane was determined by filtering four different types of salt solutions, and the retentions are shown in Figure 6. As expected for a

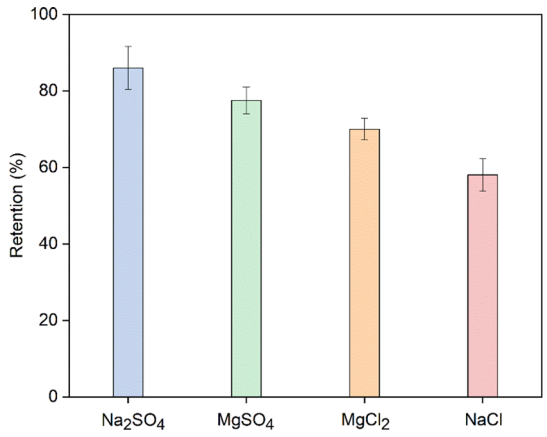

Figure 6. Salt retentions of the TFC membranes. Retention tests were conducted using 5 mM salt solution at a feed pressure of 4 bar.

negatively charged dense membrane, the rejection of Na_2SO_4 is the highest, i.e., ~86%. $MgSO_4$ and $MgCl_2$ are ~77.5 and ~70% retained by the TFC membrane. The least rejection was for NaCl, which was only ~58% retained. The retentions of salts are in accordance with the Donnan exclusion mechanism. A thin polyamide coating successfully transformed an ultrafiltration type membrane into a dense nanofiltration type membrane.

The major difference between the LBL approach for PEM assembly and the IP in this work is the thickness and density of the final surface coating. Most IP coatings are known to be ~100to 300 nm thick,[50] but PEM coatings are typically thinner, ~50 nm. A thicker selective layer increases the resistance for the water molecules, consequently resulting in lower pure water permeabilities as observed for the TFC membranes in this work. Both the PEM and IP coatings have advantages and disadvantages. The coating process is longer in PEMs, while IP is fairly easy and takes considerably less time and is still the preferred option for commercial applications. Additionally, the excess amine groups in the APS support membrane could covalently bind the IP layer for a better adhesion. In this work, we have added APS membranes to the list of supports that can be used to perform functional coatings without any pretreatment processes. Future efforts could also be devoted toward developing and optimizing these coatings for reverse osmosis and gas separation applications using the sustainably produced APS membranes as the support.

4. CONCLUSIONS

For the first time, we have successfully demonstrated that APS-based membranes can act as excellent supports for fabricating nanofiltration type membranes with thin selective top layers. PEM assembly and IP were employed to fabricate thin films on the surface of PSS-PAH APS membranes. The APS membranes were used as supports to coat different multilayers composed of three pairs of polyelectrolytes, i.e., PSS-PAH, PSS-PDADMAC, and PSS-PEI. The results revealed that by simply coating 4.5 bilayers of PEMs, the APS support membranes can be transformed into nanofiltration type membranes with excellent salt retentions and water permeabilities. The membranes coated using PSS-PAH had an MWCO of ~392 Da, while those prepared using PSS-PDADMAC had an MWCO of ~384 Da. These membranes showed decent rejections of salts, e.g., >90% $MgCl_2$ rejections. The PSS-PEI membranes were found to have the densest top layers with an MWCO of ~205 Da and rejected ~98% $MgCl_2$ with rejections of organic micropollutants in excess of 90%. The IP coating was also very successful in transforming the ultrafiltration type PSS-PAH APS membranes into nanofiltration type ones. The resulting TFC membranes had a significantly denser structure and lower MWCO of ~200 Da with good retentions of salts. The APS support membranes even have natural advantages: their charge allows for easy application of PEMs, while the used primary amines allow

https://doi.org/10.1021/acsapm.1c00457
ACS Appl. Polym. Mater. 2021, 3, 3560−3568

covalent bonding of the IP layer. Here, we also show that the properties of APS membranes can be further fine-tuned to obtain desirable separation performances.

■ ASSOCIATED CONTENT

Supporting Information

The Supporting Information is available free of charge at https://pubs.acs.org/doi/10.1021/acsapm.1c00457.

Pure water permeability and salt retention of PSS-PAH, PSS-PDADMAC, and PSS-PEI multilayer membranes showing the effect of the number of bilayers; sieving curves to determine the molecular weight cut-off of membranes; chemical structures of the organic micropollutants; comparison of PWP and NaCl retention of commercial membranes and APS-based membranes (PDF)

■ AUTHOR INFORMATION

Corresponding Author

Wiebe M. de Vos − *Faculty of Science and Technology, Membrane Science and Technology, MESA+ Institute for Nanotechnology, University of Twente, 7500 AE Enschede, The Netherlands;* orcid.org/0000-0002-0133-1931; Email: w.m.devos@utwente.nl

Authors

Muhammad Irshad Baig − *Faculty of Science and Technology, Membrane Science and Technology, MESA+ Institute for Nanotechnology, University of Twente, 7500 AE Enschede, The Netherlands*

Joshua D. Willott − *Faculty of Science and Technology, Membrane Science and Technology, MESA+ Institute for Nanotechnology, University of Twente, 7500 AE Enschede, The Netherlands;* orcid.org/0000-0003-1870-755X

Complete contact information is available at: https://pubs.acs.org/10.1021/acsapm.1c00457

Notes

The authors declare no competing financial interest.

■ ACKNOWLEDGMENTS

This work was supported by the European Research Council (ERC) under the European Union's Horizon 2020 research and innovation program (ERC StG 714744 SAMBA). W.d.V. and J.D.W. acknowledge funding support from the "Vemieuwingsimpuls" programme through project VIDI 723.015.003 (financed by the Netherlands Organization for Scientific Research, NWO).

■ REFERENCES

(1) Nunes, S. P.; Culfaz-Emecen, P. Z.; Ramon, G. Z.; Visser, T.; Koops, G. H.; Jin, W.; Ulbricht, M. Thinking the Future of Membranes: Perspectives for Advanced and New Membrane Materials and Manufacturing Processes. *J. Membr. Sci.* **2020**, *598*, 117761.

(2) Kim, D.; Nunes, S. P. Green Solvents for Membrane Manufacture: Recent Trends and Perspectives. *Curr. Opin. Green Sustain. Chem.* **2021**, *28*, 100427.

(3) Willott, J. D.; Nielen, W.; de Vos, W. M. Stimuli-Responsive Membranes through Sustainable Aqueous Phase Separation. *ACS Appl. Polym. Mater.* **2020**, *2*, 659−667.

(4) Nielen, W. M.; Willott, J. D.; de Vos, W. M. Aqueous Phase Separation of Responsive Copolymers for Sustainable and Mechanically Stable Membranes. *ACS Appl. Polym. Mater.* **2020**, *2*, 1702−1710.

(5) Sadman, K.; Delgado, D. E.; Won, Y.; Wang, Q.; Gray, K. A.; Shull, K. R. Versatile and High-Throughput Polyelectrolyte Complex Membranes via Phase Inversion. *ACS Appl. Mater. Interfaces* **2019**, *11*, 16018−16026.

(6) Durmaz, E. N.; Baig, M. I.; Willott, J.; de Vos, W. M. Polyelectrolyte Complex Membranes via Salinity Change Induced Aqueous Phase Separation. *ACS Appl. Polym. Mater.* **2020**, *2*, 2612−2621.

(7) Kamp, J.; Emonds, S.; Borowec, J.; Restrepo Toro, M. A.; Wessling, M. On the Organic Solvent Free Preparation of Ultrafiltration and Nanofiltration Membranes Using Polyelectrolyte Complexation in an All Aqueous Phase Inversion Process. *J. Membr. Sci.* **2021**, *618*, 118632.

(8) Baig, M. I.; Durmaz, E. N.; Willott, J. D.; de Vos, W. M. Sustainable Membrane Production through Polyelectrolyte Complexation Induced Aqueous Phase Separation. *Adv. Funct. Mater.* **2020**, *30*, 1907344.

(9) Baig, M. I.; Willott, J. D.; de Vos, W. M. Tuning the Structure and Performance of Polyelectrolyte Complexation Based Aqueous Phase Separation Membranes. *J. Membr. Sci.* **2020**, *615*, 118502.

(10) Baig, M. I.; Sari, P. P. I.; Li, J.; Willott, J. D.; de Vos, W. M. Sustainable Aqueous Phase Separation Membranes Prepared through Mild PH Shift Induced Polyelectrolyte Complexation of PSS and PEI. *J. Membr. Sci.* **2021**, *625*, 119114.

(11) Durmaz, E. N.; Willott, J. D.; Fatima, A.; de Vos, W. M. Weak Polyanion and Strong Polycation Complex Based Membranes: Linking Aqueous Phase Separation to Traditional Membrane Fabrication. *Eur. Polym. J.* **2020**, *139*, 110015.

(12) Mavukkandy, M. O.; McBride, S. A.; Warsinger, D. M.; Dizge, N.; Hasan, S. W.; Arafat, H. A. Thin Film Deposition Techniques for Polymeric Membranes− A Review. *J. Membr. Sci.* **2020**, *610*, 118258.

(13) Ghosh, A. K.; Jeong, B. H.; Huang, X.; Hoek, E. M. V. Impacts of Reaction and Curing Conditions on Polyamide Composite Reverse Osmosis Membrane Properties. *J. Membr. Sci.* **2008**, *311*, 34−45.

(14) Jeong, B.-H.; Hoek, E. M. V.; Yan, Y.; Subramani, A.; Huang, X.; Hurwitz, G.; Ghosh, A. K.; Jawor, A. Interfacial Polymerization of Thin Film Nanocomposites: A New Concept for Reverse Osmosis Membranes. *J. Membr. Sci.* **2007**, *294*, 1−7.

(15) Wei, J.; Liu, X.; Qiu, C.; Wang, R.; Tang, C. Y. Influence of Monomer Concentrations on the Performance of Polyamide-Based Thin Film Composite Forward Osmosis Membranes. *J. Membr. Sci.* **2011**, *381*, 110−117.

(16) Song, Y.; Sun, P.; Henry, L.; Sun, B. Mechanisms of Structure and Performance Controlled Thin Film Composite Membrane Formation via Interfacial Polymerization Process. *J. Membr. Sci.* **2005**, *251*, 67−79.

(17) Gohil, J. M.; Ray, P. A Review on Semi-Aromatic Polyamide TFC Membranes Prepared by Interfacial Polymerization: Potential for Water Treatment and Desalination. *Sep. Purif. Technol.* **2017**, *181*, 159−182.

(18) Tsai, C. W.; Tsai, C.; Ruaan, R. C.; Hu, C. C.; Lee, K. R. Interfacially Polymerized Layers for Oxygen Enrichment: A Method to Overcome Robeson's Upper-Bound Limit. *ACS Appl. Mater. Interfaces* **2013**, *5*, 5563−5568.

(19) Lee, J.; Doherty, C. M.; Hill, A. J.; Kentish, S. E. Water Vapor Sorption and Free Volume in the Aromatic Polyamide Layer of Reverse Osmosis Membranes. *J. Membr. Sci.* **2013**, *425-426*, 217−226.

(20) Yao, Z.; Guo, H.; Yang, Z.; Lin, C.; Zhu, B.; Dong, Y.; Tang, C. Y. Reactable Substrate Participating Interfacial Polymerization for Thin Film Composite Membranes with Enhanced Salt Rejection Performance. *Desalination* **2018**, *436*, 1−7.

(21) Li, X.; Li, Q.; Fang, W.; Wang, R.; Krantz, W. B. Effects of the Support on the Characteristics and Permselectivity of Thin Film Composite Membranes. *J. Membr. Sci.* **2019**, *580*, 12−23.

(22) Karami, P.; Khorshidi, B.; McGregor, M.; Peichel, J. T.; Soares, J. B. P.; Sadrzadeh, M. Thermally Stable Thin Film Composite

Polymeric Membranes for Water Treatment: A Review. *J. Cleaner Prod.* **2020**, *250*, 119447.
(23) Decher, G. Fuzzy Nanoassemblies: Toward Layered Polymeric Multicomposites. *Science* **1997**, *277*, 1232−1237.
(24) Schlenoff, J. B.; Dubas, S. T. Mechanism of Polyelectrolyte Multilayer Growth: Charge Overcompensation and Distribution. *Macromolecules* **2001**, *34*, 592−598.
(25) Joseph, N.; Ahmadiannamini, P.; Hoogenboom, R.; Vankelecom, I. F. J. Layer-by-Layer Preparation of Polyelectrolyte Multilayer Membranes for Separation. *Polym. Chem.* **2014**, *5*, 1817−1831.
(26) Ariga, K.; Hill, J. P.; Ji, Q. Layer-by-Layer Assembly as a Versatile Bottom-up Nanofabrication Technique for Exploratory Research and Realistic Application. *Phys. Chem. Chem. Phys.* **2007**, *9*, 2319−2340.
(27) Li, X.; Liu, C.; Van Der Bruggen, B. Polyelectrolytes Self-Assembly: Versatile Membrane Fabrication Strategy. *J. Mater. Chem. A* **2020**, *8*, 20870−20896.
(28) Ng, L. Y.; Mohammad, A. W.; Ng, C. Y.; Leo, C. P.; Rohani, R. Development of Nanofiltration Membrane with High Salt Selectivity and Performance Stability Using Polyelectrolyte Multilayers. *Desalination* **2014**, *351*, 19−26.
(29) Schmitt, J.; Gruenewald, T.; Decher, G.; Pershan, P. S.; Kjaer, K.; Loesche, M. Internal Structure of Layer-by-Layer Adsorbed Polyelectrolyte Films: A Neutron and X-Ray Reflectivity Study. *Macromolecules* **1993**, *26*, 7058−7063.
(30) Shan, W.; Bacchin, P.; Aimar, P.; Bruening, M. L.; Tarabara, V. V. Polyelectrolyte Multilayer Films as Backflushable Nanofiltration Membranes with Tunable Hydrophilicity and Surface Charge. *J. Membr. Sci.* **2010**, *349*, 268−278.
(31) Hong, S. U.; Malaisamy, R.; Bruening, M. L. Optimization of Flux and Selectivity in Cl-/SO42- Separations with Multilayer Polyelectrolyte Membranes. *J. Membr. Sci.* **2006**, *283*, 366−372.
(32) Hong, S. U.; Ouyang, L.; Bruening, M. L. Recovery of Phosphate Using Multilayer Polyelectrolyte Nanofiltration Membranes. *J. Membr. Sci.* **2009**, *327*, 2−5.
(33) Reurink, D. M.; Willott, J. D.; Roesink, H. D. W.; De Vos, W. M. Role of Polycation and Cross-Linking in Polyelectrolyte Multilayer Membranes. *ACS Appl. Polym. Mater.* **2020**, *2*, 5278−5289.
(34) DuChanois, R. M.; Epsztein, R.; Trivedi, J. A.; Elimelech, M. Controlling Pore Structure of Polyelectrolyte Multilayer Nanofiltration Membranes by Tuning Polyelectrolyte-Salt Interactions. *J. Membr. Sci.* **2019**, *581*, 413−420.
(35) Ilyas, S.; Abtahi, S. M.; Akkilic, N.; Roesink, H. D. W.; de Vos, W. M. Weak Polyelectrolyte Multilayers as Tunable Separation Layers for Micro-Pollutant Removal by Hollow Fiber Nanofiltration Membranes. *J. Membr. Sci.* **2017**, *537*, 220−228.
(36) te Brinke, E.; Achterhuis, I.; Reurink, D. M.; de Grooth, J.; de Vos, W. M. Multiple Approaches to the Buildup of Asymmetric Polyelectrolyte Multilayer Membranes for Efficient Water Purification. *ACS Appl. Polym. Mater.* **2020**, *2*, 715−724.
(37) Chen, Y.; Xiangli, F.; Jin, W.; Xu, N. Streaming Potential Characterization of LBL Membranes on Porous Ceramic Supports. *AIChE J.* **2007**, *53*, 969−977.
(38) Ormanci-Acar, T.; Mohammadifakhr, M.; Benes, N. E.; de Vos, W. M. Defect Free Hollow Fiber Reverse Osmosis Membranes by Combining Layer-by-Layer and Interfacial Polymerization. *J. Membr. Sci.* **2020**, *610*, 118277.
(39) Hong, S. U.; Miller, M. D.; Bruening, M. L. Removal of Dyes, Sugars, and Amino Acids from NaCl Solutions Using Multilayer Polyelectrolyte Nanofiltration Membranes. *Ind. Eng. Chem. Res.* **2006**, *45*, 6284−6288.
(40) Krasemann, L.; Tieke, B. Selective Ion Transport across Self-Assembled Alternating Multilayers of Cationic and Anionic Polyelectrolytes. *Langmuir* **2000**, *16*, 287−290.
(41) Boom, R. M.; Wienk, I. M.; van den Boomgaard, T.; Smolders, C. A. Microstructures in Phase Inversion Membranes. Part 2. The Role of a Polymeric Additive. *J. Membr. Sci.* **1992**, *73*, 277−292.
(42) Donnan, F. G. Theory of Membrane Equilibria and Membrane Potentials in the Presence of Non-Dialysing Electrolytes. A Contribution to Physical-Chemical Physiology. *J. Membr. Sci.* **1995**, *100*, 45−55.
(43) Verliefde, A.; Cornelissen, E.; Amy, G.; Van der Bruggen, B.; van Dijk, H. Priority Organic Micropollutants in Water Sources in Flanders and the Netherlands and Assessment of Removal Possibilities with Nanofiltration. *Environ. Pollut.* **2007**, *146*, 281−289.
(44) Anand, A.; Unnikrishnan, B.; Mao, J. Y.; Lin, H. J.; Huang, C. C. Graphene-Based Nanofiltration Membranes for Improving Salt Rejection, Water Flux and Antifouling−A Review. *Desalination* **2018**, *429*, 119−133.
(45) Benbow, N. L.; Webber, J. L.; Pawliszak, P.; Sebben, D. A.; Ho, T. T. M.; Vongsvivut, J.; Tobin, M. J.; Krasowska, M.; Beattie, D. A. A Novel Soft Contact Piezo-Controlled Liquid Cell for Probing Polymer Films under Confinement Using Synchrotron FTIR Microspectroscopy. *Sci. Rep.* **2018**, *8*, 17804.
(46) Itano, K.; Choi, J.; Rubner, M. F. Mechanism of the PH-Induced Discontinuous Swelling/Deswelling Transitions of Poly(Allylamine Hydrochloride)-Containing Polyelectrolyte Multilayer Films. *Macromolecules* **2005**, *38*, 3450−3460.
(47) Prakash Rao, A.; Joshi, S. V.; Trivedi, J. J.; Devmurari, C. V.; Shah, V. J. Structure-Performance Correlation of Polyamide Thin Film Composite Membranes: Effect of Coating Conditions on Film Formation. *J. Membr. Sci.* **2003**, *211*, 13−24.
(48) Tang, C. Y.; Kwon, Y. N.; Leckie, J. O. Effect of Membrane Chemistry and Coating Layer on Physiochemical Properties of Thin Film Composite Polyamide RO and NF Membranes. I. FTIR and XPS Characterization of Polyamide and Coating Layer Chemistry. *Desalination* **2009**, *242*, 149−167.
(49) Liu, S.; Wu, C.; Hung, W. S.; Lu, X.; Lee, K. R. One-Step Constructed Ultrathin Janus Polyamide Nanofilms with Opposite Charges for Highly Efficient Nanofiltration. *J. Mater. Chem. A* **2017**, *5*, 22988−22996.
(50) Veerababu, P.; Vyas, B. B.; Singh, P. S.; Ray, P. Limiting Thickness of Polyamide-Polysulfone Thin-Film-Composite Nanofiltration Membrane. *Desalination* **2014**, *346*, 19−29.

https://doi.org/10.1021/acsapm.1c00457
ACS Appl. Polym. Mater. 2021, 3, 3560−3568